## Title

Human von Economo Neurons Express Transcription Factors Associated with Layer V Subcerebral Projection Neurons



## Journal

Cerebral Cortex, 25(1)

## ISSN

1047-3211

## Authors

Cobos, Inma
Seeley, William W

## Publication Date

2015

## DOI

10.1093/cercor/bht219

Peer reviewed

Cerebral Cortex January 2015;25:213–220
doi:10.1093/cercor/bht219
Advance Access publication August 19, 2013

# Human von Economo Neurons Express Transcription Factors Associated with Layer V Subcerebral Projection Neurons

Inma Cobos[1,2] and William W. Seeley[1]

[1]Memory and Aging Center, Department of Neurology, University of California, San Francisco, CA 94158, USA and
[2]Current address: Department of Pathology, Massachusetts General Hospital, 55 Fruit Street, Boston, MA 02114, USA

Address correspondence to William W. Seeley; Email: wseeley@memory.ucsf.edu

**The von Economo neurons (VENs) are large bipolar Layer V projection neurons found chiefly in the anterior cingulate and frontoinsular cortices. Although VENs have been linked to prevalent illnesses such as frontotemporal dementia, autism, and schizophrenia, little is known about VEN identity, including their major projection targets. Here, we undertook a developmental transcription factor expression study, focusing on markers associated with specific classes of Layer V projection neurons. Using mRNA in situ hybridization, we found that VENs prominently express FEZF2 and CTIP2, transcription factors that regulate the fate and differentiation of subcerebral projection neurons, in humans aged 3 months to 65 years. In contrast, few VENs expressed markers associated with callosal or corticothalamic projections. These findings suggest that VENs may represent a specialized Layer V projection neuron for linking cortical autonomic control sites to brainstem or spinal cord regions.**

**Keywords:** anterior insula, axon targeting, cell identity, molecular specification, neuronal connectivity

## Introduction

Current frameworks for understanding neuronal identity and laminar fate specification in the cerebral cortex have the potential to shed light on neuropsychiatric disorders that feature a vulnerability gradient across neuronal subtypes. The von Economo neurons (VENs), large bipolar Layer V projection neurons found primarily in anterior cingulate (ACC) and frontoinsular (FI) cortices, have been shown to undergo early, selective degeneration in frontotemporal dementia (FTD; Seeley et al. 2006, 2012; Seeley 2008, 2010; Kim et al. 2012), and some evidence points to VEN abnormalities in autism and schizophrenia (Simms et al. 2009; Brüne et al. 2010; Santos et al. 2011). VENs had previously been identified only in large-brained mammals from distant lineages (apes, humans, cetaceans, and elephants), but recent findings suggest that VENs are present in 2 commonly used laboratory primates, macaca mulatta and macaca fasicularis (Evrard et al. 2012), making studies of VEN hodology feasible for the first time.

VEN identity remains sparsely characterized, including whether the morphologically similar neurons classified as VENs across species share distinctive molecular or connectivity profiles. VENs are filled retrogradely after injections of the carbocyanine dye DiI into the cingulum bundle, show high nonphosphorylated neurofilament levels, lack calcium-binding protein expression, and express the kidney-type glutaminase isoform of the phosphate-activated glutaminase, suggesting that they are excitatory glutamatergic projection neurons (Nimchinsky et al. 1995; Allman et al. 2010, 2011; Evrard et al. 2012). VENs differ from neighboring Layer V pyramidal neurons, however, in size, morphology, ontogeny, and phylogeny. For instance, VENs cannot be identified morphologically until gestational week 36 (Allman et al. 2010), although neurogenesis of human Layer V pyramidal neurons is estimated to take place between gestational weeks 6.5 and 10 (Bayer and Altman 2007). As neuronal birth and laminar fate are controlled by highly conserved developmental mechanisms, VENs may represent an unusual Layer V pyramidal neuron specialization.

Tools to explore these diverse facets of VEN identity have begun to arise within developmental neuroscience. In utero, neuronally expressed transcription factors presage neuronal destiny, especially with regard to laminar fate and axonal projection targets. We reasoned that a developmental study of VEN transcription factor expression might help clarify the identity of these fascinating and clinically relevant neurons. To focus the analyses, we took a candidate-based approach, studying transcription factors expressed, to varying degrees, by Layer V projection neurons (i.e., SOX5, TBR1, FEZF2, CTIP2, LMO4, and FOXP1) and the chromatin-remodeling factor SATB2 (Arlotta et al. 2005; Molyneaux et al. 2007; Kwan et al. 2008; Lai et al. 2008; Leone et al. 2008; Bedogni et al. 2010; Cederquist et al. 2013), seeking to provide a preliminary categorization of VENs with regard to their likely projection targets. Genetic studies in mice have shown that cross-regulatory interactions between FEZF2, CTIP2, SATB2, and TBR1 regulate neuronal subtype specification in Layer V, largely via repression of alternative fates. For instance, FEZF2 is necessary and sufficient for the differentiation of layer V neurons that project subcortically to the striatum, superior colliculus, basal pons, and spinal cord; CTIP2 is a major downstream effector of FEZF2 (Chen et al. 2008; Rouaux and Arlotta 2010). SATB2 expression determines callosal projections, and the segregation of subcortical and callosal projections in Layer V relies on the repression of SATB2 expression by FEZF2 and repression of CTIP2 expression by SATB2 (Alcamo et al. 2008; Srinivasan et al. 2012). SATB2-positive callosal projection neurons coexpress FOXP1 and LMO4 (Azim et al. 2009; Hisaoka et al. 2010). TBR1 promotes the identity of corticothalamic neurons and inhibits subcerebral fates, primarily through repressing FEZF2 and CTIP2 transcription (Han et al. 2011; McKenna et al. 2011). Accordingly, FEZF2/CTIP2, SATB2 and TBR1 are commonly used in mouse cortex as markers for subcerebral, callosal, and corticothalamic neuronal identities, respectively. Our analysis shows that nearly all mature VENs in human FI and ACC express high levels of the subcerebral projection neuron markers FEZF2 and CTIP2, suggesting that VENs represent a large, specialized Layer V projection neuron whose predominant targets will be found below the cerebrum.

## Methods

### *Postmortem Human Brain Tissue*

All human brain tissues were provided by the NICHD Brain and Tissue Bank for Developmental Disorders at the University of Maryland, Baltimore, and their use for this study was approved by the University of California at San Francisco Committee on Human Research. We studied brain tissues from 6 subjects, aged 18 days, 100 days, 2 years, 6 years, 32 years, and 65 years. All subjects lacked a clinical history of neurological symptoms or brain injury, and postmortem neuropathological assessment revealed a brain lacking gross pathological changes.

Fresh-frozen tissue blocks from the 2 VEN-rich brain regions, the ACC and FI, were used for mRNA in situ hybridization. All fresh-frozen samples were obtained from the left hemisphere, with the exception of the 6-year-old subject. Formalin-fixed tissue blocks taken from the contralateral ACC and FI were examined in parallel to provide familiarity with VEN morphology in individual subjects across the diverse age span studied. Postmortem interval ranged from 7 to 22 h. pH ranged from 6.6 to 6.9, and RNA integrity numbers in the cerebral cortex ranged from 6.8 to 7.1 among subjects for whom this information was available from the brain bank. Ultimate tissue suitability was determined by performing in situ hybridization pilot studies to confirm mRNA detection and by examining adjacent Nissl-stained sections to confirm the region of interest (ACC and FI), the presence of VENs, and the absence of severe freezing artifacts.

### *Histology, Immunohistochemistry, and RNA in Situ Hybridization*

Fresh-frozen tissue was embedded in Tissue-Tek OCT compound (Sakura), cut at 20 μm thickness on a cryostat, and mounted on Fisher Superfrost/Plus slides for RNA in situ hybridization, double fluorescence in situ hybridization and immunohistochemistry, and Nissl staining. Formalin-fixed tissue was sectioned at 50 or 100 μm on a sliding microtome and used for free-floating immunohistochemistry and Nissl staining.

Standard in situ hybridization methods (Palop et al. 2011) were optimized for human fresh-frozen brain tissue. Briefly, the cryostat sections were air-dried for 20 min and fixed with 4% paraformaldehyde in phosphate-buffered saline solution (0.1 M, pH 7.4) for 30 min. Then, sections were briefly digested with proteinase K for 5 min, acetylated, and incubated in hybridization buffer [50% formamide, 5× salt sodium citrate (SSC) buffer, pH 7.0, 5× Denhardt's solution, 0.25 mg/mL salmon sperm DNA, 0.5 mg/mL yeast tRNA) for 3–4 h at room temperature. The slides were incubated horizontally with hybridization buffer containing the digoxigenin-labeled antisense riboprobe (typically at a concentration of 200–400 ng/mL) in a slide humidity incubation box at 68 °C for approximately 16 h. Posthybridization stringent wash conditions (i.e., low salt concentration, 0.2× saline-sodium citrate buffer, and high temperature, 68 °C) helped to reduce nonspecific binding of probes. The detection of the digoxigenin-labeled RNA probes was done by immunohistochemistry with antidigoxigenin antibodies conjugated to alkaline phosphatase (1:3000, Roche). The in situ-labeled RNA was visualized by light microscopy using a colorimetric detection reagent (5-bromo-4-chloro-3-indolyl-phosphate and nitro blue tetrazolium chromogen) or by fluorescence microscopy using the HNPP/Fast Red TR chromogen.

The RNA digoxigenin probes used were synthesized from human expressed sequence tag clones (Open Biosystems) that were specific for the gene of interest: SOX5 (BE467463), TBR1 (AW026499), FEZF2 (BM807621), CTIP2 (BG697939), SATB2 (AA393182), LMO4 (AI952998), and FOXP1 (AI183585). Our expression data were largely in agreement with published human and mouse expression data and the Allen brain atlas public electronic database (http://www.brain-map.org/).

For combined fluorescence RNA in situ hybridization and immunohistochemistry on frozen sections, the immunohistochemistry was carried out after the in situ hybridization following standard protocols (Palop et al. 2011). Monoclonal mouse anti-NeuN (1:500; Chemicon) and rabbit monoclonal anti-Satb2 (1:1000; clone number EPNCIR130, Abcam) antibodies were used. Goat antimouse or goat antirabbit fluorescent secondary antibodies, conjugated with Alexa 488 (1:200; Molecular Probes), were used. Immunohistochemistry to detect MAP2 on free-floating 50 or 100 μm thick sections was performed according to standard methods using the antibody mouse anti-MAP2 (2a + 2b; 1:500, Sigma).

Nonstereological counting was used to quantify the percentage of VENs expressing a given transcription factor in Layer Vb of the ACC and FI. We chose a nonstereological quantitative approach because of the relatively low abundance of VENs in the tissue and the thin nature of our sections (20 μm prior to drying), which precludes true stereological estimates since only a single optical focal plane can be resolved. Counts were performed on representative digitized images obtained with a digital camera connected to a Nikon upright fluorescence microscope, using a ×40 objective. All slides were counted by a single examiner blinded to the subject and marker (I.C.). Digitized images were used to define the field of counted cells, and the examiner focused through the captured field and changed magnification as needed to confirm cellular morphology and VEN identity. Selected slides were independently confirmed by a second examiner (W.W.S.) with regard to anatomical context, VEN location and morphology, and the approximate proportion of VENs expressing each marker. Ten specimens from 5 different subjects (6 samples from the ACC, and 4 from the FI) were analyzed. For each specimen and marker, 3–6 cryostat sections were analyzed. Overall, at least 50 VENs were analyzed for each specimen and marker. NeuN immunohistochemistry served to visualize VENs and to distinguish them from neighboring Layer V pyramidal neurons, based on the large and elongated VEN soma and single basal dendrite (Watson et al. 2006). In situ hybridization signal was read as either positive or negative for each individual VEN. In some instances (i.e., SATB2, TBR1), low and high expression levels of transcripts could be clearly distinguished and were annotated. All sections were counterstained with 4′,6-diamidino-2-phenylindole (DAPI) (Vectashield® Hard Set™ mounting medium with DAPI, Vector Laboratories) to provide cytoarchitectural context. Some specimens, particularly the ones from aged brains, showed a degree of autofluorescence due to lipofuscin accumulation. Lipofuscin autofluorescent signal was granular and homogeneous, located in the cytoplasm, and emitted a yellow fluorescence when excited with ultraviolet or blue light; these features were dissimilar to the more diffuse, nuclear in situ hybridization signal, allowing clear discrimination between true-positive signal from transcription factor mRNA and false-positive autofluorescent signal due to lipofuscin.

## Results

### *Layer-Specific Expression of SOX5, TBR1, FEZF2, CTIP2, SATB2, LMO4, and FOXP1 in Human Anterior Cingulate and Frontoinsular Cortices*

ACC and FI are agranular transition zones between periallocortex and pro-isocortex. They feature an absent Layer IV, inconspicuous Layer II, and a prominent Layer V, sublaminated into Va and Vb. Having confirmed these cytoarchitectural features with Nissl staining in all tissue samples examined, we used in situ hybridization to characterize expression patterns of 6 transcription factors, SOX5, TBR1, FEZF2, CTIP2, LMO4, and FOXP1, and the chromatin-remodeling factor SATB2, implicated in the control of cerebral cortex laminar fate and the generation of deep layer projection neurons (Molyneaux et al. 2007; Leone et al. 2008). We studied the ACC and FI of early postnatal (age 18 and 100 days), late postnatal (age 2 and 6 years), and adult (age 32 and 65 years) human brains (Figs 1–3). Although previous human studies have described the cortical expression of some of these genes (Hevner 2007; Ip et al. 2011; Saito et al. 2011), details on their spatio-temporal expression in human ACC and FI are lacking.

SOX5 and TBR1 expression were present in deep layers VI and V (Figs 1 and 2 and not shown). TBR1 showed highest expression in Layer VI, with only a few scattered neurons in Layer V and lower diffuse expression throughout Layers II–IV

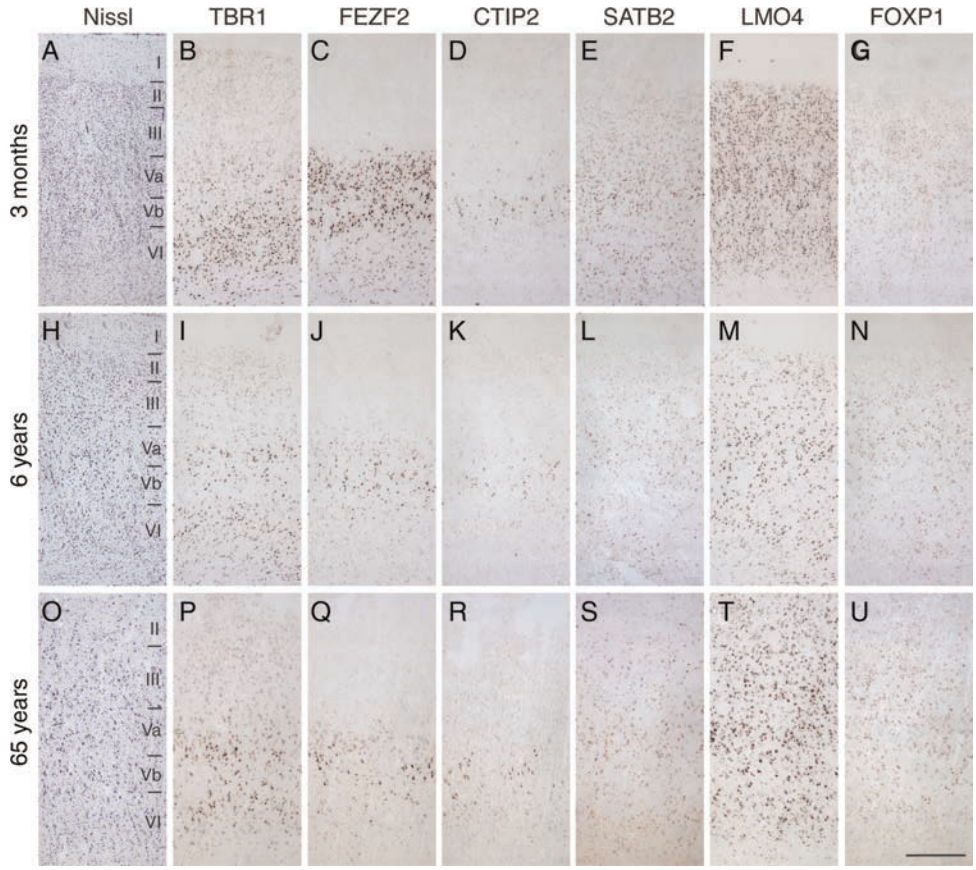


**Figure 1.** Transcription factor expression profiles in human anterior cingulate cortex. (*A–U*) In situ mRNA hybridization of TBR1, FEZF2, CTIP2, SATB2, LMO4, and FOXP1 in adjacent sections through the ACC from 3-month- (*A–G*), 6-year- (*H–N*), and 65-year-old (*O–U*) subjects. TBR1 is highly expressed by Layer VI neurons. High levels of FEZF2 and CTIP2 were detected in Layer Vb. SATB2, LMO4, and FOXP1 show broader expression across Layers VI–II. Note the maintenance of gene expression patterns across the age span examined. Scale bar: 500 μm.

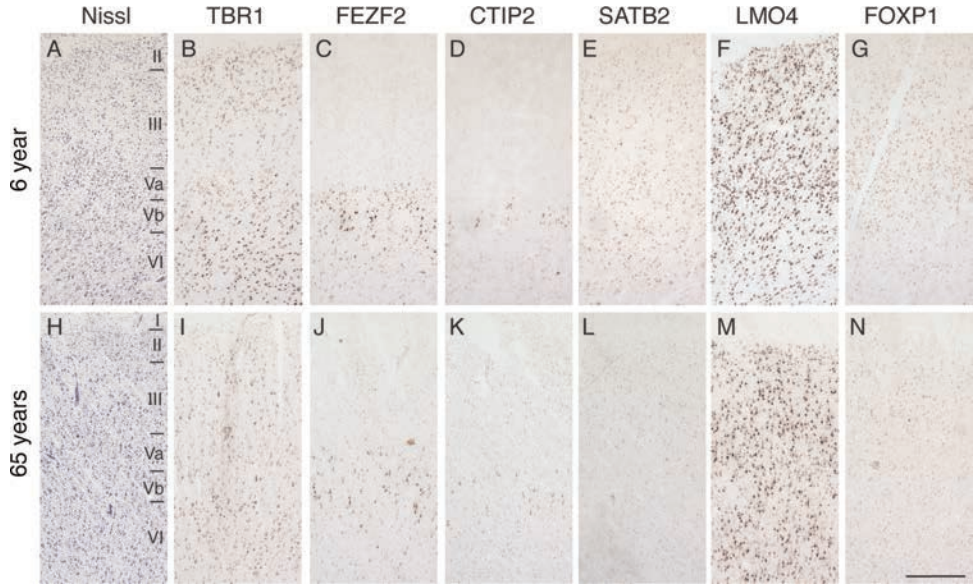


**Figure 2.** Transcription factor expression profiles in human frontoinsula. (*A–N*) In situ mRNA hybridization of TBR1, FEZF2, CTIP2, SATB2, LMO4, and FOXP1 in adjacent sections through the frontoinsula from 6-year- (*A–G*) and 65-year-old (*H–N*) subjects. The laminar pattern of transcription factor expression strongly resembled that seen in the ACC (Fig. 1). Scale bar: 500 μm.

(Figs 1*B*,*I*,*P* and 2*B*,*I*). FEZF2 and CTIP2 were also expressed in Layers VI and V, but compared with TBR1 they showed highest expression in Layer Vb and lower expression in Layer VI. Comparing these markers, CTIP2 expression occupied a more restricted pattern than FEFZ2, with CTIP2-expressing neurons found in Layers Vb and VI, but not in Layer Va

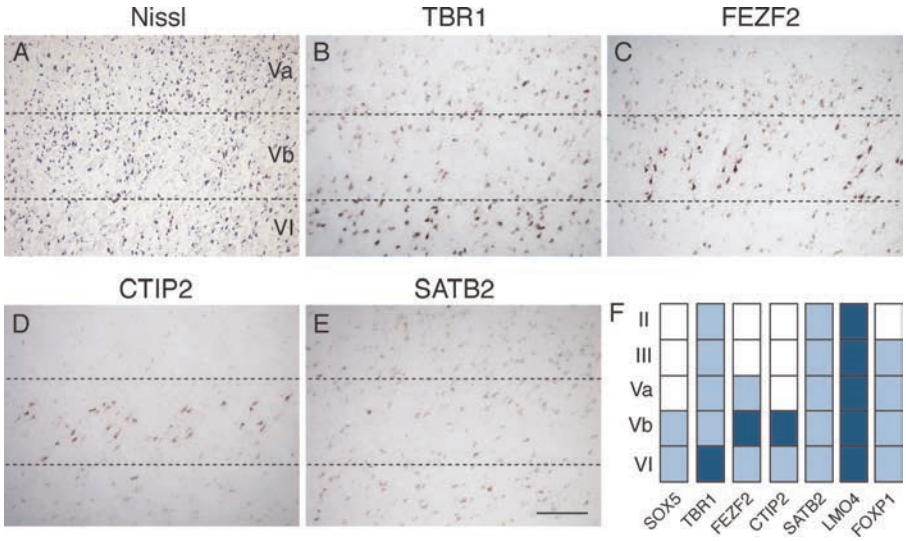


**Figure 3.** Transcription factor expression in Layer Vb of human frontoinsula. (*A–E*) Nissl staining and in situ mRNA hybridization of TBR1, FEZF2, CTIP2, and SATB2 in adjacent sections through the frontoinsula of a 6-year-old subject. Note the presence of FEZF2- and CTIP2-high expressing neurons in Layer Vb, at times in clusters. Scattered neurons expressing SATB2 and TBR1 are also detected in Layer Vb. (*F*) Graph summarizing the distinct laminar expression of SOX5, TBR1, FEZF2, CTIP2, SATB2, LMO4, and FOXP1 mRNA in human ACC/frontoinsula. Blue color indicates transcription factor expression; light or dark blue indicate low or high expression levels, respectively. Dashed lines indicate approximate boundaries between cortical layers. Scale bar: 200 μm.

(Figs 1 and 2). SATB2 and LMO4 were expressed diffusely across Layers II–VI, without obvious laminar specificity at any of the ages analyzed (Figs 1 and 2). FOXP1 was expressed in Layers III–VI, with the highest expression in Layer III (Figs 1*G*, *N*,*U* and 2*G*,*N*).

Because the great majority of VENs are located in cortical Layer Vb, we focused our analysis on this region. When comparing the expression of TBR1, FEZF2, CTIP2, and SATB2 within Layer Vb, clusters of large neurons that were FEZF2- and CTIP2-positive were observed (Fig. 3*A*,*C*,*D*). Infrequent TBR1-positive neurons were also present in Layer Vb, albeit with lower expression levels than those seen in Layer VI neurons (Fig. 3*B*). The majority of Layer Vb neurons showed low expression of SATB2, although occasional high expression was observed in scattered neurons (Fig. 3*E*).

In summary, our analysis identified restricted expression patterns of SOX5, TBR1, FEZF2, and CTIP2 in deep Layers V/VI, with TBR1 showing prominent expression in Layer VI, and FEZF2/CTIP2 in Layer Vb. In contrast, SATB2, LMO4, and FOXP1 expression patterns spanned Layers II–VI (Fig. 3*F*). Notably, these expression patterns were established at early postnatal stages (i.e., 3 months of age, Fig. 1*A–G*) and maintained into the aging brain (i.e., 65 years of age, Figs 1*O–U* and 2*H–N*) in ACC and FI (Fig. 3*F*).

### *VENs Express High Levels of FEZF2 and CTIP2 and low Levels of SATB2*

VENs are concentrated in Layer Vb of the ACC and FI, and some are singly found in Layer Va (Allman et al. 2010). At present, VEN-specific cellular or molecular markers are lacking; therefore, VEN identification relies on distinguishing VENs by their large and elongated bipolar somata and their thick and rather symmetrical apical and basal dendrites (Fig. 4*A*; Watson et al. 2006). In situ hybridization for FEZF2 and CTIP2 revealed large neurons with an elongated morphology reminiscent of VENs in Layer Vb, at postnatal and adult ages (Fig. 4*B*,*C* and not shown). Double fluorescence in situ hybridization for FEZF2 and immunohistochemistry for NeuN confirmed the expression of FEZF2 in neurons with the distinctive VEN morphology (Fig. 4*D*). In contrast, such neurons in Layer V expressed low albeit detectable levels of SATB2 transcripts. A few scattered neurons with relatively small and round somata in Layer V showed conspicuous SATB2 expression (Fig. 4*E*). Double fluorescence in situ hybridization for FEZF2 and immunohistochemistry for SATB2 revealed complimentary expression of the 2 markers, such that cells with high levels of one marker showed low levels of the other. Double fluorescence immunohistochemistry for SATB2 and in situ hybridization for SATB2 showed similar distribution of the protein and the mRNA, at postnatal and adult stages (not shown). Thus, these results are consistent with VENs expressing high levels of FEZF2 and CTIP2 and low levels of SATB2.

To quantify the percentage of VENs expressing TBR1, FEZF2, CTIP2, SATB2, and LMO4, we performed double fluorescence in situ hybridization for each of these genes and immunohistochemistry for NeuN in ACC and FI from subjects aged 3 months to 6 years (Fig. 5). At 3 months of age, neurons with typical VEN morphology showed no expression of TBR1, whereas FEZF2 and CTIP2 were detected in approximately 45–55%, SATB2 was detected at low levels in approximately 33%, and LMO4 was detected in approximately 15% (Fig. 5*A*,*G*). In the 6-year-old subject, a small percentage of VENs (~10%) appeared to express TBR1, virtually all VENs expressed FEZF2, CTIP2, and LMO4, and approximately 33% of VENs expressed low levels of SATB2. Thus, our analysis showed that all or nearly all mature VENs in human FI and ACC express FEZF2 and CTIP2 at relatively high levels, whereas about one-third of VENs express SATB2, albeit at lower levels. A small percentage of VENs expresses TBR1. LMO4 expression is prominent in VENs, but also in nearly all putative projection neurons across Layers II–VI. This transcription factor expression profile suggests a subcerebral projection neuron identity and raises the possibility that a subset of human VENs may send secondary projections intracortically (Table 1).

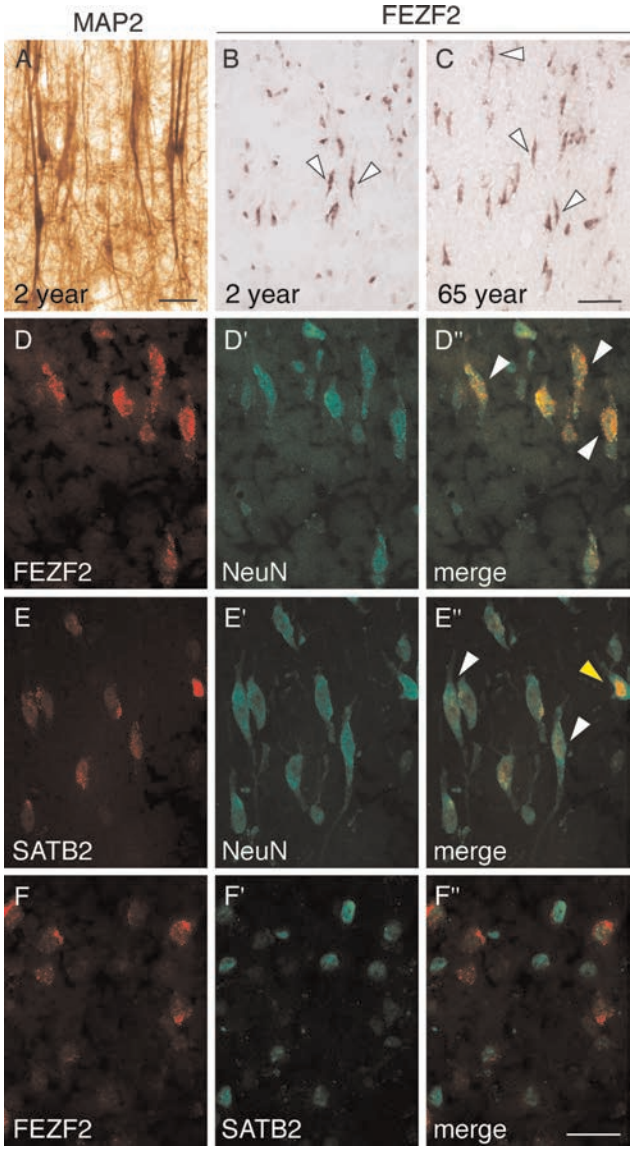


**Figure 4.** VENs express high levels of FEZF2 and low levels of SATB2. (*A*) MAP2 immunohistochemistry highlighting the bipolar morphology of VENs in a representative 50 μm thick formalin-fixed section of the frontoinsula from a 2-year-old subject. (*B* and *C*) In situ mRNA hybridization of FEZF2 in 20 μm thick fresh-frozen sections through the ACC from a 2-year- and a 65-year-old subject. White arrowheads point to FEZF2-positive neurons with an elongated soma and a single basal dendrite, resembling VENs. (*D–E″*) Double fluorescence in situ mRNA hybridization for either FEZF2 or SATB2 (red) and immunohistochemistry for NeuN (green) in representative sections through the frontoinsula from a 6-year-old subject. White arrowheads in *D″* point to presumed FEZF2-positive VENs. White arrowheads in *E″* point to presumed SATB2-low expressing VENs, whereas the yellow arrowhead points to a SATB2-high expressing small round neuron. (*F′F″*) Double fluorescence in situ mRNA hybridization for FEZF2 (red) and immunohistochemistry for SATB2 (green) in a representative section through the frontoinsula from a 6-year-old subject. Note the absence of colocalization between FEZF2-high expressing neurons and SATB2-high expressing neurons. Scale bars: *A* 50 μm; *B* and *C* 100 μm; *D–F″* 50 μm.

## Discussion

VENs represent a population of disease-relevant Layer V projection neurons found only in ACC and FI. Here, we studied the molecular identity of the VENs within a developmental neuroscience framework, demonstrating that VENs express FEZF2 and CTIP2, transcription factors essential for the specification of Layer V subcerebral projection neurons. Substantial mouse genetic evidence has shown that FEZF2 is a master gene necessary and sufficient for the differentiation of Layer V neurons that project to the striatum, superior colliculus, basal pons, and spinal cord, whereas CTIP2 is a major downstream effector of FEZF2 (Chen et al. 2008; Rouaux and Arlotta 2010; Shim et al. 2012; De la Rossa et al. 2013). The FEZF2–CTIP2 genetic pathway executes the subcerebral identity largely through mutual repression with SATB2, a promoter of callosal identity, as well as mutual repression with TBR1, a promoter of corticothalamic identity (Alcamo et al. 2008; Han et al. 2011; McKenna et al. 2011; Srinivasan et al. 2012). Remarkably, when FEZF2 is ectopically expressed in early postmitotic Layer II/III callosal projection neurons, these are reprogrammed to acquire the molecular identity and axonal connectivity of subcerebral projection neurons (Rouaux and Arlotta 2013). Our data show robust FEZF2 and CTIP2 expression in human VENs emerging within the first year of life and continuing into late adulthood, consistent with roles in establishing and maintaining a subcerebral projection phenotype.

It is intriguing that although virtually all VENs express high levels of FEZF2 and CTIP2, a subset (~33%) of VENs co-expressed low levels of SATB2, and scarce (10%) VENs expressed TBR1. The expression of SATB2 in mice determines callosal projection identity (Alcamo et al. 2008; Britanova et al. 2008). TBR1 determines the corticothalamic projection fate in Layer VI neurons, although its relatively lower expression in Layers II/III and scattered cells within Layer V appears to regulate the callosal fate downstream of SATB2 (Srinivasan et al. 2012). Thus, human VENs may be a heterogeneous population comprising projection neurons with diverse targets including the contralateral cortex. Ultimately, how all these genes interact with repressor complexes to fine tune transcription levels and ultimately to shape the final projection identities of VENs is unclear and needs to be addressed experimentally. For instance, it is unclear whether the subset of VENs co-expressing high levels of FEZF2/CTIP2 and low levels of SATB2 may send projecting fibers exclusively to subcortical areas or additionally target intracortical areas. The present work may serve as a guide for future axonal tracer studies that seek to identify VEN projection targets in the macaque.

To which subcerebral regions might VENs project? This question, though not addressed by the present work, has become tractable in light of the recent discovery that cynomolgus and rhesus macaques, both commonly used in axonal tracing experiments, possess VENs in the ACC and FI. Evrard et al. (2012) reported retrograde labeling of scant right FI VENs after Alexa 594 dextran injection into the left FI. These authors also reported left FI VEN filling after left dorsal midinsula injection. These preliminary findings suggest that a subset of VENs may send a callosal axon that connects the VEN populations within the homologous structures of the 2 hemispheres. This hypothesis aligns with our observation that some VENs express a low level of the callosal marker SATB2. Our data, however, suggest that the search for VEN projection targets should include subcortical and subcerebral structures known to receive inputs from the ACC and ventral anterior agranular insula in monkeys. Candidate targets include, but need not be limited to, regions that participate in autonomic–visceral–nociceptive processing, such as the amygdala, hypothalamus, periaqueductal gray matter, parabrachial nucleus,

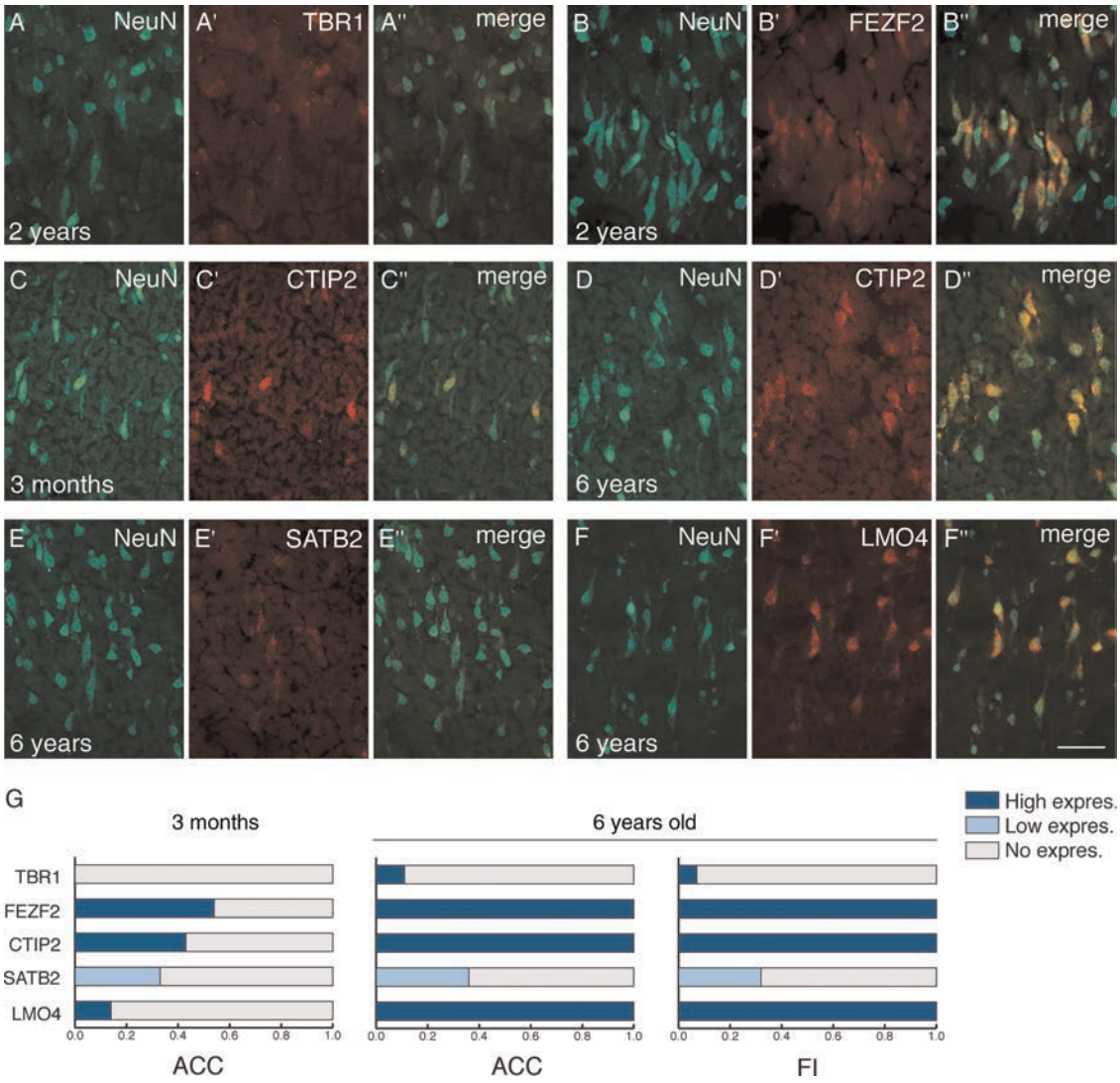


**Figure 5.** Patterns of transcription factor expression in Layer Vb VENs. (*A–F″*) Double fluorescence in situ mRNA hybridization for TBR1, FEZF2, CTIP2, SATB2, and LMO4 (red) and immunohistochemistry for NeuN (green) in representative sections of the ACC or frontoinsula from 3-month-, 2-year-, and 6-year-old subjects. High magnification views of Layer Vb are shown. NeuN immunohistochemistry was used to identify VENs and distinguish them from neighboring pyramidal neurons. Yellow arrowheads point to VENs expressing FEZF2, CTIP2, SATB2, or LMO4; white arrowheads point to VENs not expressing TBR1 or SATB2. (*G*) Percentage of VENs expressing TBR1, FEZF2, CTIP2, SATB2, and LMO4 in Layer Vb of the ACC or frontoinsula from 3-month- and 6-year-old subjects. Blue indicates transcription factor expression; light or dark shades indicate low or high expression levels. TBR1 is expressed in a small proportion of VENs (~10%) at age of 6 years. FEZF2 and CTIP2 are detected in approximately 45–55% of VENs at 3 months of age, and in virtually all VENs at 6 years of age. SATB2 is detected, albeit at low levels, in 30–40% of VENs. LMO4 is detected in virtually all NeuN-positive neurons at 6 years, including VENs and pyramidal neurons. Scale bar: 100 μm.

**Table 1**
TBR1, FEZF2, CTIP2, SATB2, and LMO4 expression in cortical projection neurons and in VENs and corresponding projection targets as demonstrated by genetically engineered mice

| | Lamina-specific expression in mouse | Lamina-specific expression in human ACC/FI | VEN expression | Projections in mice | References |
|---|---|---|---|---|---|
| TBR1 | II–VI (highest in VI) | II–VI (highest in VI) | Scattered cells (~10%) | Corticothalamic Callosal[a] | Bedogni et al. (2010); Srinivasan et al. (2012) |
| FEZF2 | V–VI (highest in Vb) | V–VI (highest in Vb) | High (100%) | Subcerebral | Chen et al. (2008); Rouaux and Arlotta (2010); Han et al. (2011); McKenna et al. (2011) |
| CTIP2 | Vb–VI (highest in Vb) | Vb–VI (highest in Vb) | High (100%) | Subcerebral | Chen et al. (2008): Rouaux and Arlota (2010); Han et al. (2011); McKenna et al. (2011) |
| SATB2 | II–VI | II–VI | Low (~33%) | Callosal | Alcamo et al. (2008); Britanova et al. (2008) |
| LMO4 | II–VI[b] | II–VI | High (100%) | Callosal Subcerebral[b] | Azim et al. (2009); Cederquist et al. (2013) |

Note: The lamina-specific expression patterns in human ACC/FI (present study) resemble those described in mouse cortex (references in right column). All VENs express high levels of the subcerebral projection markers FEZF2 and CTIP2, while a subset of VENs expresses low levels of the callosal marker SATB2. Scattered VENs express TBR1.
[a]High TBR1 expression in Layer VI determines the corticothalamic projection fate, while its lower expression in Layer II/III and V appears to regulate the callosal fate downstream of SATB2 (Srinivasan et al. 2012).
[b]LMO4 shows area-specific expression; in mouse rostral motor cortex it is expressed by both subcerebral and callosal projection neurons (Cederquist et al. 2013).

nucleus of the solitary tract, nucleus ambiguus, and the dorsal motor nucleus of the vagus nerve. Incorporating molecular classification approaches into macaque VEN hodological studies may further inform the conservation of projection target specification mechanisms across mammals.

Future studies will need to determine whether VENs represent a homogenous population that forms a single narrow and targeted projection or an assembly of morphologically similar neurons with diverse projection targets. To address this question may require multiple retrograde tracer injections within a single organism and multicolor in situ hybridization and immunohistochemistry approaches to decode the "molecular logic" (Woodworth et al. 2012; Custo Greig et al. forthcoming; Macklis personal communication) guiding individual VEN identity. A related question regards whether individual VEN axons may branch in order to reach multiple targets. This possibility would reconcile our observation that all or most VENs express transcription factors associated with subcerebral projection neurons with the evidence that some VENs project across the corpus callosum (Evrard et al. 2012).

VEN integrity has been studied in several neuropsychiatric disorders (Seeley et al. 2006; Brüne et al. 2010; Santos et al. 2011; Kim et al. 2012; Santillo et al. 2013), and the present findings can be viewed within the context of working functional–anatomical disease models. VEN loss has been perhaps most convincingly demonstrated in behavioral variant FTD (bvFTD), a neurodegenerative disorder in which the ACC and FI represent early targets (Seeley et al. 2008). Consistent with the hypothesis that VENs project to subcerebral regions, patients with bvFTD show early loss of intrinsic functional connectivity within the "salience network," a neural system anchored by ACC and FI in which patients show disrupted connectivity to subcortical and brainstem nodes of the network (Zhou et al. 2010).

## Funding

This work was supported by the James S. McDonnell Foundation and by NIH grant AG033017.

## Notes

Human tissue was obtained from the NICHD Brain and Tissue Bank for Developmental Disorders at the University of Maryland, Baltimore, MD. The Bank is funded by NIH (contract no. #HHSN275200900011C and ref. no. NO1-HD-9-0011). *Conflict of Interest*: None declared.

## References

Alcamo EA, Chirivella L, Dautzenberg M, Dobreva G, Fariñas I, Grosschedl R, McConnell SK. 2008. Satb2 regulates callosal projection neuron identity in the developing cerebral cortex. Neuron. 57(3):364–377.

Allman JM, Tetreault NA, Hakeem AY, Manaye KF, Semendeferi K, Erwin JM, Park S, Goubert V, Hof PR. 2011. The von Economo neurons in the frontoinsular and anterior cingulate cortex. Ann N Y Acad Sci. 1225:59–71.

Allman JM, Tetreault NA, Hakeem AY, Manaye KF, Semendeferi K, Erwin JM, Park S, Goubert V, Hof PR. 2010. The von Economo neurons in frontoinsular and anterior cingulate cortex in great apes and humans. Brain Struct Funct. 214(5–6):495–517.

Arlotta P, Molyneaux BJ, Chen J, Inoue J, Kominami R, Macklis JD. 2005. Neuronal subtype-specific genes that control corticospinal motor neuron development in vivo. Neuron. 45(2):207–221.

Azim E, Shnider SJ, Cederquist GY, Sohur US, Macklis JD. 2009. Lmo4 and Clim1 progressively delineate cortical projection neuron subtypes during development. Cereb Cortex. 19(Suppl 1):i62–i69.

Bayer SA, Altman J. 2007. Timespans of neurogenesis. In: The human brain during the early first trimester, 1st ed. Boca Raton, Florida: CRC Press. p. 490–497.

Bedogni F, Hodge RD, Elsen GE, Nelson BR, Daza RA, Beyer RP, Bammler TK, Rubenstein JL, Hevner RF. 2010. Tbr1 regulates regional and laminar identity of postmitotic neurons in developing neocortex. Proc Natl Acad Sci USA. 107(29):13129–13134.

Britanova O, de Juan Romero C, Cheung A, Kwan KY, Schwark M, Gyorgy A, Vogel T, Akopov S, Mitkovski M, Agoston D et al. 2008. Satb2 is a postmitotic determinant for upper-layer neuron specification in the neocortex. Neuron. 57(3):378–392.

Brüne M, Schöbel A, Karau R, Benali A, Faustmann PM, Juckel G, Petrasch-Parwez E. 2010. Von Economo neuron density in the anterior cingulate cortex is reduced in early onset schizophrenia. Acta Neuropathol. 119(6):771–778.

Cederquist GY, Azim E, Shnider SJ, Padmanabhan H, Macklis JD. 2013. Lmo4 establishes rostral motor cortex projection neuron subtype diversity. J Neurosci. 33(15):6321–6332.

Chen B, Wang SS, Hattox AM, Rayburn H, Nelson SB, McConnell SK. 2008. The Fezf2-Ctip2 genetic pathway regulates the fate choice of subcortical projection neurons in the developing cerebral cortex. Proc Natl Acad Sci USA. 105(32):11382–11387.

Custo Greig LF, Woodworth MB, Galazo MJ, Padmanabhan HK, Macklis JD. Forthcoming 2013. Molecular logic of neocortical projection neuron specification and development. Nat Rev Neurosci. doi: 10.1038/nrn3586.

De la Rossa A, Bellone C, Golding B, Vitali I, Moss J, Toni N, Lüscher C, Jabaudon D. 2013. In vivo reprogramming of circuit connectivity in postmitotic neocortical neurons. Nat Neurosci. 16(2):193–200.

Evrard HC, Forro T, Logothetis NK. 2012. Von Economo neurons in the anterior insula of the macaque monkey. Neuron. 74(3):482–489.

Han W, Kwan KY, Shim S, Lam MM, Shin Y, Xu X, Zhu Y, Li M, Sestan N. 2011. TBR1 directly represses Fezf2 to control the laminar origin and development of the corticospinal tract. Proc Natl Acad Sci USA. 108(7):3041–3046.

Hevner RF. 2007. Layer-specific markers as probes for neuron type identity in human neocortex and malformations of cortical development. J Neuropathol Exp Neurol. 66(2):101–109.

Hisaoka T, Nakamura Y, Senba E, Morikawa Y. 2010. The forkhead transcription factors, Foxp1 and Foxp2, identify different subpopulations of projection neurons in the mouse cerebral cortex. Neuroscience. 166(2):551–563.

Ip BK, Bayatti N, Howard NJ, Lindsay S, Clowry GJ. 2011. The corticofugal neuron-associated genes ROBO1, SRGAP1, and CTIP2 exhibit an anterior to posterior gradient of expression in early fetal human neocortex development. Cereb Cortex. 21(6):1395–1407.

Kim EJ, Sidhu M, Gaus SE, Huang EJ, Hof PR, Miller BL, DeArmond SJ, Seeley WW. 2012. Selective frontoinsular von Economo neuron and fork cell loss in early behavioral variant frontotemporal dementia. Cereb Cortex. 22(2):251–259.

Kwan KY, Lam MM, Krsnik Z, Kawasawa YI, Lefebvre V, Sestan N. 2008. SOX5 postmitotically regulates migration, postmigratory differentiation, and projections of subplate and deep-layer neocortical neurons. Proc Natl Acad Sci USA. 105(41):16021–6.

Lai T, Jabaudon D, Molyneaux BJ, Azim E, Arlotta P, Menezes JR, Macklis JD. 2008. SOX5 controls the sequential generation of distinct corticofugal neuron subtypes. Neuron. 57(2):232–247.

Leone DP, Srinivasan K, Chen B, Alcamo E, McConnell SK. 2008. The determination of projection neuron identity in the developing cerebral cortex. Curr Opin Neurobiol. 18(1):28–35.

McKenna WL, Betancourt J, Larkin KA, Abrams B, Guo C, Rubenstein JL, Chen B. 2011. Tbr1 and Fezf2 regulate alternate corticofugal neuronal identities during neocortical development. J Neurosci. 31(2):549–564.

Molyneaux BJ, Arlotta P, Menezes JR, Macklis JD. 2007. Neuronal subtype specification in the cerebral cortex. Nat Rev Neurosci. 8(6):427–437.

Nimchinsky EA, Vogt BA, Morrison JH, Hof PR. 1995. Spindle neurons of the human anterior cingulate cortex. J Comp Neurol. 355(1):27–37.

Palop JJ, Roberson ED, Cobos I. 2011. Step-by-step in situ hybridization method for localizing gene expression changes in the brain. Methods Mol Biol. 670:207–230.

Rouaux C, Arlotta P. 2013. Direct lineage reprogramming of post-mitotic callosal neurons into corticofugal neurons in vivo. Nat Cell Biol. 15(2):214–221.

Rouaux C, Arlotta P. 2010. Fezf2 directs the differentiation of corticofugal neurons from striatal progenitors in vivo. Nat Neurosci. 13 (11):1345–1347.

Saito T, Hanai S, Takashima S, Nakagawa E, Okazaki S, Inoue T, Miyata R, Hoshino K, Akashi T, Sasaki M et al. 2011. Neocortical layer formation of human developing brains and lissencephalies: consideration of layer-specific marker expression. Cereb Cortex. 21 (3):588–596.

Santillo AF, Nilsson C, Englund E. 2013. Von Economo neurons are selectively targeted in frontotemporal dementia. Neuropathol Appl Neurobiol. doi:10.1111/nan.12021.

Santos M, Uppal N, Butti C, Wicinski B, Schmeidler J, Giannakopoulos P, Heinsen H, Schmitz C, Hof PR. 2011. Von Economo neurons in autism: a stereologic study of the frontoinsular cortex in children. Brain Res. 1380:206–217.

Seeley WW. 2010. Anterior insula degeneration in frontotemporal dementia. Brain Struct Funct. 214(5–6):465–475.

Seeley WW. 2008. Selective functional, regional, and neuronal vulnerability in frontotemporal dementia. Curr Opin Neurol. 21(6):701–707.

Seeley WW, Carlin DA, Allman JM, Macedo MN, Bush C, Miller BL, Dearmond SJ. 2006. Early frontotemporal dementia targets neurons unique to apes and humans. Ann Neurol. 60(6):660–667.

Seeley WW, Crawford R, Rascovsky K, Kramer JH, Weiner M, Miller BL, Gorno-Tempini ML. 2008. Frontal paralimbic network atrophy in very mild behavioral variant frontotemporal dementia. Arch Neurol. 65(2):249–255.

Seeley WW, Merkle FT, Gaus SE, Craig AD, Allman JM, Hof PR, Economo CV. 2012. Distinctive neurons of the anterior cingulate and frontoinsular cortex: a historical perspective. Cereb Cortex. 22 (2):245–250.

Shim S, Kwan KY, Li M, Lefebvre V, Sestan N. 2012. Cis-regulatory control of corticospinal system development and evolution. Nature. 486(7401):74–79.

Simms ML, Kemper TL, Timbie CM, Bauman ML, Blatt GJ. 2009. The anterior cingulate cortex in autism: heterogeneity of qualitative and quantitative cytoarchitectonic features suggests possible subgroups. Acta Neuropathol. 118(5):673–684.

Srinivasan K, Leone DP, Bateson RK, Dobreva G, Kohwi Y, Kohwi-Shigematsu T, Grosschedl R, McConnell SK. 2012. A network of genetic repression and derepression specifies projection fates in the developing neocortex. Proc Natl Acad Sci USA. 109 (47):19071–19078.

Watson KK, Jones TK, Allman JM. 2006. Dendritic architecture of the von Economo neurons. Neuroscience. 141(3):1107–1112.

Woodworth MB, Custo Greig L, Kriegstein AR, Macklis JD. 2012. Snapshot: cortical development. Cell. 151(4):918.

Zhou J, Greicius MD, Gennatas ED, Growdon ME, Jang JY, Rabinovici GD, Kramer JH, Weiner M, Miller BL, Seeley WW. 2010. Divergent network connectivity changes in behavioural variant frontotemporal dementia and Alzheimer's disease. Brain. 133(Pt 5):1352–1367.